Available online at www.sciencedirect.com
SCIENCE DIRECT
Polymer 47 (2006) 1715–1721
polymer
www.elsevier.com/locate/polymer

High birefringence of poly(trimethylene terephthalate) spherulite

Jong Hwa Yun, Keiichi Kuboyama *, Toshiaki Ougizawa

Department of Organic and Polymeric Materials, Tokyo Institute of Technology, 2-12-1-S8-33, Ookayama, Meguro-Ku, Tokyo 152-8552, Japan

Received 5 August 2005; received in revised form 5 December 2005; accepted 11 December 2005
Available online 19 January 2006

Abstract

Poly(trimethylene terephthalate) (PTT) spherulite shows interference color under polarized light microscope without a sensitive tint plate. The fact indicates that the retardation of PTT spherulite is high, while it was reported that the birefringence in PTT fiber is low. In this study, the reason why the high birefringence is observed in PTT spherulite was discussed. By small area X-ray diffraction measurement, it was confirmed that *a*-axis of unit cell of PTT crystal was parallel to the radial direction of the spherulite. Based on the result, we calculated the refractive indices of parallel to *a*-axis and the other orthogonal directions. It was clarified that the refractive index of *a*-axis is much lower than the others and the intrinsic birefringence for *a*-axis orientation is high. It is the reason why the PTT spherulite shows high and negative birefringence.

Keywords: Poly(trimethylene terephthalate); Spherulite; Intrinsic birefringence

1. Introduction

Poly(trimethylene terephthalate) (PTT) is a semicrystalline polyester, which has three methylene groups in the backbone [1]. The study on PTT was much fewer than that of the similar polyesters, poly(ethylene terephthalate) (PET) and poly(butylene terephthalate) (PBT) until the middle of 1990s because the production cost of PTT was much more expensive than the other polyesters. However, PTT has come to be used industrially due to the lowering of production cost and then can be easily obtained commercially in last decade. In such a situation, the investigations on PTT spherulite and fiber have increased in these several years. For PTT spherulite, morphology and crystallization kinetics have been reported. Large spherulite with diameter ranging from several micrometers to a few milimeters can be easily obtained in PTT and shows a banded spherulite in a certain crystallization temperature range [2].

Moreover, it was reported that the PTT spherulite shows vivid interference color under polarized light microscope (PLM) without a sensitive tint plate [3]. The interference color under PLM is known as follows. First, the birefringence Δn_s in a spherulite is described as the equation:

$$\Delta n_s = n_r - n_t, \tag{1}$$

where n_r and n_t are the refractive indices of parallel and tangential to the radial direction, respectively. In case that the light passes through the material with birefringence Δn and thickness d, the retardation R is given by

$$R = \Delta n d. \tag{2}$$

Birefringent material shows interference color under cross-Nicol condition depending on the retardation of the material. In spherulites of many polymers, however, colors observed under PLM are black and white because of the low retardation [4,5]. A sensitive tint plate with retardation of 530 nm is usually used to observe the color for such a low retardation sample and it is located between the polarizing plates where the angle between polarizing axis of polarizing plates and one of the principal axes of the tint plate is 45°. Considering these conditions, the fact that the interference color can be observed in PTT spherulite under PLM without a sensitive tint plate indicates that the spherulite has relatively high birefringence. However, there are few reports about the birefringence of PTT spherulite [3], while there are several studies on the birefringence of PTT fiber. The birefringence of PTT fiber is lower than that of the other similar polyesters (PET, PBT) and the values of highly oriented PTT is about 0.05 [6–9], while the values of PET and PBT (α-crystal) are more than 0.2 and 0.155, respectively [10,11]. There are only a few reports on the intrinsic birefringence of PTT crystal in fiber. The values of crystalline phase reported in the two reports were 0.029 and 0.206, respectively [12,13]. These values are completely

* Corresponding author. Tel./fax: +81 3 5734 2439.
E-mail address: kkuboyam@o.cc.titech.ac.jp (K. Kuboyama).

0032-3861/$ - see front matter © 2005 Published by Elsevier Ltd.
doi:10.1016/j.polymer.2005.12.067

different. The former is the calculated one under the assumption that *c*-axis of PTT unit cell is parallel to one of the principal axes of refractive indices. On the other hand, the latter is the experimentally estimated one for PTT drawn filament, however, the measured values used for estimating the intrinsic birefringence varied widely and then the error of the estimated value was considerably large. As described above, there are not enough researches for the birefringence of PTT even in fiber.

This paper describes the reason why the isothermally melt crystallized PTT spherulite shows the high birefringence. The orientation direction of the PTT unit cell was estimated by small area X-ray diffraction measurement of PTT spherulite. The intrinsic birefringence in the spherulite was calculated based on both the result of the small area X-ray diffraction measurement and the refractive indices calculated from the crystallographic data and bond polarizabilities.

2. Experimental

PTT was supplied by Asahi Kasei Chemicals Corporation. The intrinsic viscosity of the PTT obtained from a phenol/tetrachloroethane (60/40) mixed solution at 25 °C was $[\eta] = 1.06$ ml/g.

PTT was first dried at 80 °C for 6 h under vacuum before sample preparation. The isothermally crystallized PTT thin film for PLM observation was obtained by the following process. A thin layer specimen of the thickness from about 10 to 20 μm was prepared by pressing the PTT fragment between two cover glasses at 280 °C. After the specimen was melted at 280 °C for 3 min, it was rapidly transferred onto a hot stage of 190 °C and isothermally crystalized and annealed for several minutes. After the crystallization, the sample was quenched at room temperature. The morphology of the spherulite was observed under PLM (Olympus BH-2).

For the wide-angle X-ray diffraction (WAXD) measurement, the bulk PTT sample was prepared by the same condition as that for PLM observation.

Density of the isothermally crystallized PTT was determined by using a density gradient column filled with *n*-heptane/carbon tetrachloride mixture at 25 °C. The range of the density gradient column is 1.28–1.44 g/cm^3. All samples were wetted by the liquid of composition corresponding to the upper position of the column before putting them into the column.

WAXD intensity curves of the samples were measured by using a Rigaku D/max diffractometer with a graphite-monochromatized Cu Kα radiation working at 40 kV and 40 mA at a scanning rate of 1°/min.

Small area X-ray diffraction measurement (Rigaku Rint Rapid) was performed by transmission method with a graphite-monochromatized Cu Kα radiation at 40 kV and 36 mA. The diameter of the pinhole collimator was 100 μm.

3. Results and discussion

3.1. Birefringence of PTT spherulite estimated from interference color

Fig. 1 shows PLM micrographs for PTT spherulite crystallized at 190 and 140 °C. As is previously reported [2,14], morphology of the spherulite is different depending on the crystallization temperature and a banded spherulite was observed at 190 °C while a non-banded one at 140 °C. The spherulites show the interference colors under PLM without a sensitive tint plate. Retardation of the spherulite can be estimated from the interference color chart, for example, Michel-Levy chart. From the chart, it can be suggested that the retardation of at least 300 nm is necessary for the vivid interference color. In Fig. 1(a), we can see the colors such as yellow, magenta and blue green and the interference colors correspond to the retardations of about 870, 1040 and 1250 nm, respectively which are measured by Berek compensator under PLM. The sample thickness of the spherulite crystallized at 190 °C was about 20 μm, then the birefringence of the spherulite was from about 0.04 to 0.06. In the same way, the

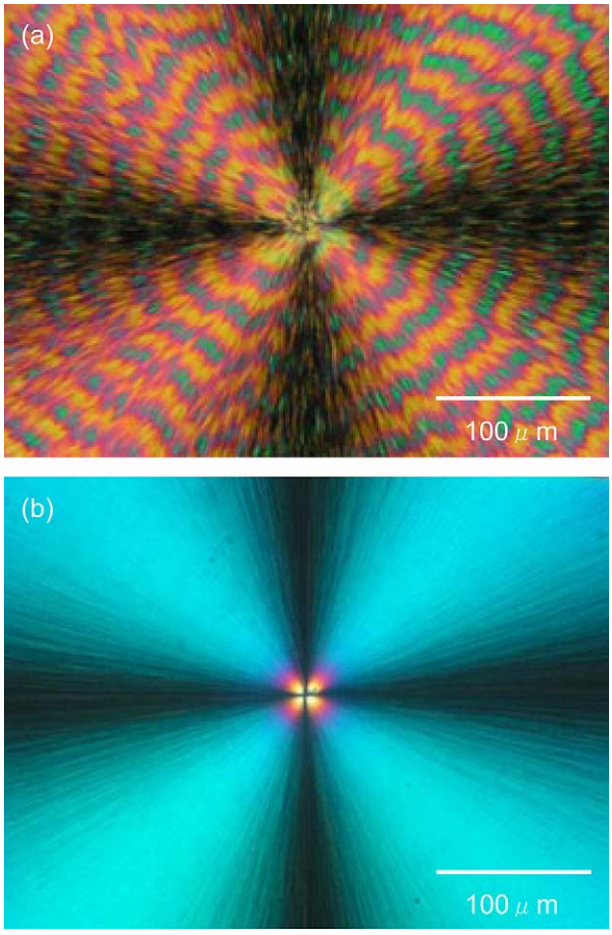

Fig. 1. PLM micrographs of PTT spherulites isothermally crystallized at (a) 190 °C and (b) 140 °C without a sensitive tint plate. Sample thickness is about 2 μm.

birefringence of sample crystallized at 140 °C could be estimated as about 0.05.

Here, when birefringence mainly originates in the crystal, birefringence of each position in a spherulite of a semicrystalline polymer Δn_s can be described by

$$\Delta n_s = \phi_{sc} f_{sc} \Delta n^0_{sc} \tag{3}$$

where ϕ_{sc} is the degree of crystallinity, f_{sc} is the degree of orientation of the molecular chain in PTT crystal with respect to the radial direction of a spherulite at each position and Δn^0_{sc} is the intrinsic birefringence of the crystallite in a spherulite and is defined as $\Delta n^0_{sc} = n_{rc} - n_{tc}$ by using the refractive indices of the crystallite of radial direction in the spherulite n_{rc} and that of transverse direction n_{tc}. In this equation, the contribution of each of the factors to the birefringence was first examined. The degrees of crystallinity of the PTT isothermally crystallized at 140 and 190 °C were estimated by two kind of measurement, that is, WAXD and crystallization temperature dependence of density measurement. The apparent degree of crystallinity X_c can be estimated by WAXD measurement using the following equation [15]:

$$X_c = \frac{A_c}{A_c + A_a} \tag{4}$$

where A_c and A_a are the sum of areas under the crystalline and amorphous peaks, respectively. The weight fraction crystallinity from density can be estimated by the following relation [16]:

$$X_c = \frac{\rho_c}{\rho} \frac{\rho - \rho_a}{\rho_c - \rho_a} \tag{5}$$

where ρ is the denstiy of the sample. The density of an ideal crystal ρ_c and amorphous ρ_a was reported to be 1.432 and 1.295 g/cm^3, respectively [17,18]. From the above two measurements, we could estimate the crystallinity of PTT spherulite as 22.3% (WAXD) and 22.0% (density) for 140 °C and 24.9% (WAXD) and 26.2% (density) for 190 °C, respectively. From the result, it was considered that the contribution of the crystallinity term in Eq. (3) was not too large for the high retardation.

The intrinsic birefringence of the PTT fiber was calculated as small value, 0.027 [12], and if that of PTT spherulite is almost the same value, the birefringence obtained from Eq. (3) is much smaller than observed value 0.05, even if the degree of orientation is assumed to be 1.0. This fact indicates that the intrinsic birefringence of the crystallite Δn^0_{sc} does not same as that of the fiber. Though the intrinsic birefringence of PTT fiber is for *c*-axis orientation, it is not possible to discuss that in the spherulite as well as in the fiber because the orientation axis of PTT unit cell in the spherulite must be different from that in the fiber. Therefore, the orientation of unit cell in PTT spherulite was first examined and then the intrinsic birefringence was calculated based on the result as described in the following subsections.

3.2. Direction of PTT unit cell orientation in spherulite

In order to calculate the birefringence of the spherulite, it is necessary to clarify the growth axis of PTT unit cell. The crystal structure of PTT has been reported by several groups for the various PTT samples crystallized under different conditions by WAXD and electron diffraction (ED) study [1,2,17,19]. PTT has only one crystalline form and the unit cell was found to be triclinic. The triclinic structure has the periodicity along the *c*-axis containing two repeat units and the flexible part with a methylene group sequence is arranged in a highly contracted *gauche–gauche* conformation [1,17]. Based on the crystal structure determined by previous studies, Chuah [12] calculated the intrinsic birefringence of PTT fiber in order to explain the low birefringence in PTT fiber. He assumed that one of the principal axes in refractive indices, *z* direction, is parallel to *c*-axis in PTT unit cell because of the small misalignment of the *c*-axis with the fiber axis. The intrinsic birefringence Δn^0_c for uniaxially oriented PTT was calculated by the following equation:

$$\Delta n^0_c = n_{zz} - \frac{n_{xx} + n_{yy}}{2}, \tag{6}$$

where n_{xx}, n_{yy} and n_{zz} are the principal refractive indices in the orthogonal coordinates under the assumption that *c*-axis is parallel to one of the principal axes. Although such an assumption may be appropriate for a fiber, it is not applicable for the spherulite and the orientation direction of PTT unit cell in the spherulite must be decided.

To clarify the direction of crystalline axes, small area X-ray diffraction measurement was performed for the isothermally crystallized PTT spherulite at 190 °C. To estimate the orientation of unit cell in a spherulite, the small area X-ray beam with diameter of 100 μm must be focused to small area inside of half side of single spherulite. Therefore, the crystallization temperature of 190 °C was chosen because large spherulite with radius of more than 100 μm can be easily obtained at the higher crystallization temperature.

Fig. 2(a) shows the schematic representation of a PTT banded spherulite and the area irradiated the small area X-ray beam for WAXD measurement. A small area X-ray beam with diameter of 100 μm was irradiated inside of one PTT spherulite and the irradiated area did not contain the center of the spherulite. The area is right-hand side of the center and then the equator and the meridian directions of the diffraction pattern by the small area X-ray beam correspond to the radial and the tangential directions of the spherulite, respectively. Fig. 2(b) shows the resulting two-dimensional diffraction pattern and the assignment of the pattern [1,17]. Moreover, the intensity profiles of meridian and equator directions are plotted in Fig. 3(a) and (b), respectively, because the anisotropy was observed in the diffraction pattern. From these figures, the reflection (010) was observed on the meridian and the weak reflection (100) was on the equator, though the reflections were diffused to the azimuth direction in Fig. 2(b) because the area irradiated the X-ray beam was relatively large compared to the scale of PTT lamella. The reflections (010) on the meridian and

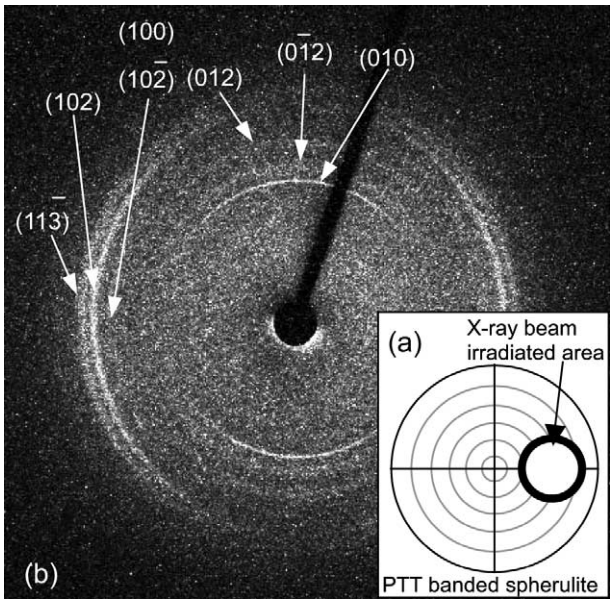

Fig. 2. Small area X-ray diffraction of PTT spherulite (sample thickness is about 50 μm). (a) Schematic representation of a PTT spherulite and the marked circle area with diameter of 100 μm inside of the spherulite is investigated area by small area X-ray diffraction measurement, (b) two-dimensional X-ray diffraction pattern.

(100) on the equator mean that *b*-axis in PTT unit cell and *a*-axis align in the direction of the meridian and the equator, respectively. In Figs. 2 and 3, the (100) reflection was much weaker than the (010), then we plotted the intensity profile of small area X-ray diffraction pattern (Fig. 2) of summation of all azimuth angles from 0 to 360° as shown in Fig. 4 and compared it with the profiles reported for the PTT powder and the fiber samples. Even though the (100) reflection was also smaller than (010) in this profile, the feature of diffraction intensity profile was similar with the other profiles measured by WAXD and ED. Moreover, Wang et al. [19] mentioned such a feature in the diffraction profile and concluded that the structure factor of (100) plane was small because the PTT chain has a big zigzag chain conformation along the *c*-axis in ac plane and then the PTT molecule is easy to deform. Therefore, the small (100) reflection in Figs. 2 and 3(b) is not the result of few existence of (100) plane but also is essential to PTT crystal.

The intensity profile of (100) and (010) reflections for azimuth angle was plotted in Fig. 5 because it was difficult to recognize whether the (100) reflection had a maximum value at equatorial direction in Fig. 2, while the (010) reflection seemed to have maximum intensity at meridian direction. It was clear that the (100) reflection took a maximum value at meridian and minimum at equator and the (010) showed the opposite feature of the (100). Considering the measured position in Fig. 2(a), the mean direction of *a*-axis in the PTT unit cell is parallel to the radial direction of spherulite and that of *b*-axis is parallel to the transverse direction to it. This result agrees with that by ED measurement [2]. However, the (102) and (10$\bar{3}$) reflections also seemed to take a maximum value at equatorial direction in Fig. 2(b). In the real spherulite (that is, not ideal one), the lamella has a distribution of

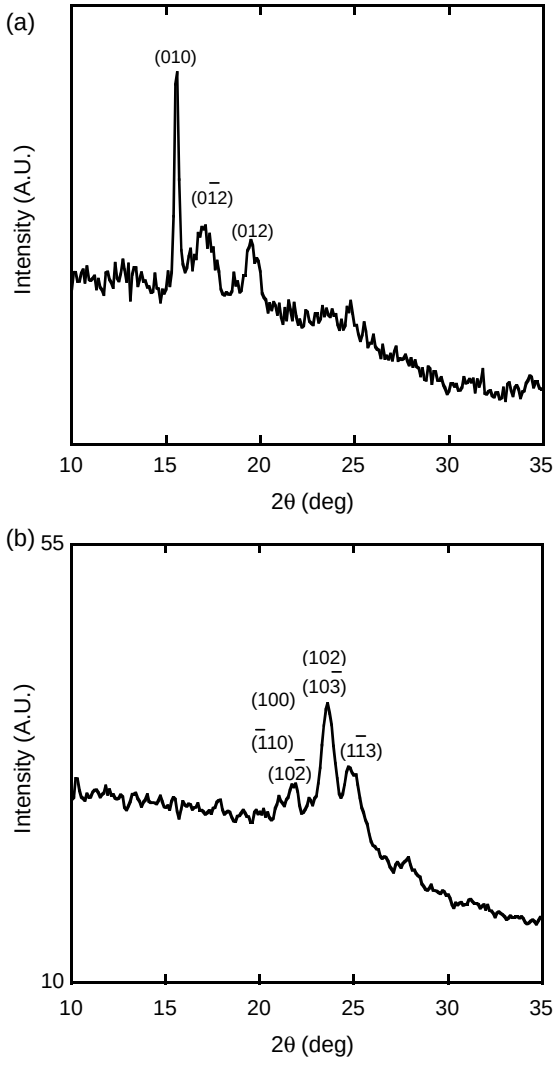

Fig. 3. Intensity profile of two-dimensional pattern at (a) meridian and (b) equator directions.

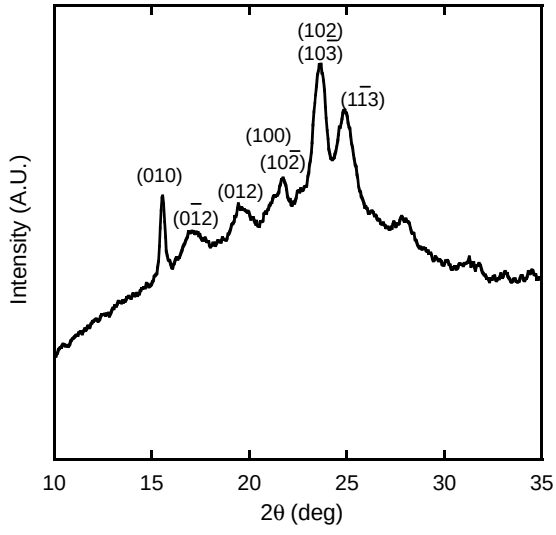

Fig. 4. Intensity profile of small area X-ray diffraction pattern of summation of all azimuth angles.

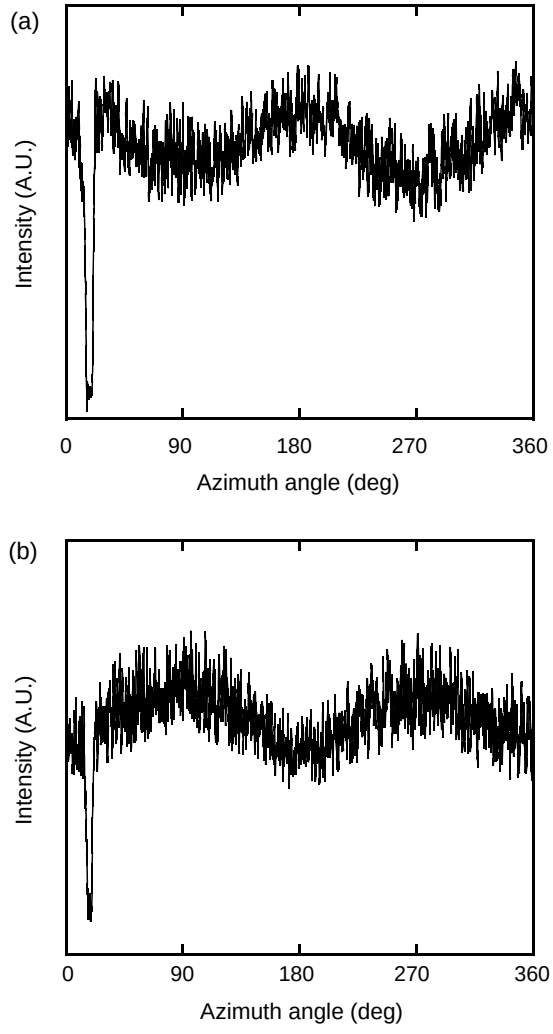

Fig. 5. Intensity profiles for azimuth angle at (a) (010) plane ($2\theta = 15.4°$) (b) (100) plane ($2\theta = 21.9°$).

orientation angle to the radial direction and it has been reported on the existence of alternating flat on and edge on morphology of lamella stack to the radial direction. Therefore, *a*-axis obviously has certain degree of distribution of misalignment with the radial direction and then the existence of the (102), $(10\bar{3})$ reflections on the equatorial direction can be explained by such a misalignment distribution of *a*-axis. However, the following calculation of the birefringence will be performed under the assumption that the lamella has an orientation parallel to the radial and *a*-axis direction for convenience.

3.3. Calculation of Δn^0_{sc}

The following Lorentz–Lorenz equation [20,21] is well known one for the relation between refractive index and molecular structure,

$$\frac{n^2-1}{n^2+2}\frac{M}{\rho_c} = \frac{4}{3}\pi N_A P, \tag{7}$$

where n is a refractive index, M is molecular weight per unit cell, ρ_c is density of crystal, N_A is Avogadro's number and P is mean polarizability. Because *a*-axis is parallel to the radial direction of the spherulite as described above, the refractive index of *a*-axis direction and the other two indices in orthogonal axes must be calculated to estimate the value of the intrinsic birefringence Δn^0_{sc}. A summation of polarizabilities in the unit cell for the three orthogonal axes can be calculated by the following equation [22],

$$P_{ij} = \sum_k \{(P_{Lk} - P_{Tk})\cos\phi_{ik}\cos\phi_{jk} + P_{Tk}I_{ij}\}, \tag{8}$$

where subscripts i and j indicate components of orthogonal coordinate (X,Y,Z), P_{Lk} and P_{Tk} are the longitudinal and transverse bond polarizabilities of each bond (k), ϕ is an angle between coordinate axis and bond axis, and I_{ij} is unit tensor, respectively. In our calculation of P_{ij}, the atomic fractional coordinates, the PTT unit cell dimensions ($a = 0.46$ nm, $b = 0.62$ nm, $c = 1.83$ nm, $\alpha = 98°$, $\beta = 90°$, $\gamma = 112°$) determined by Desborough et al. [17] and the values of longitudinal and transverse bond polarizabilities proposed by Bunn [25] were used. We defined that *X*-axis is parallel to *a*-axis, *Y*-axis is put in the *ac* plane, that is, *Y*-axis is parallel to *c*-axis because of $\beta = 90°$, and then *Z*-axis is parallel to crystallographic b^*-axis. The calculated refractive indices were $n_X = 1.528$, $n_Y = 1.643$, $n_Z = 1.754$. The principal refractive indices were given by substituting eigenvalues of polarizability tensor obtained from Eq. (8) as $n_1 = 1.524$, $n_2 = 1.634$, $n_3 = 1.767$ in ascending order and (X,Y,Z) components of the corresponding eigenvectors v_1, v_2, v_3 were

$$v_1 = \begin{pmatrix} 0.991 \\ 0.066 \\ -0.120 \end{pmatrix}, \qquad v_2 = \begin{pmatrix} -0.032 \\ 0.963 \\ 0.269 \end{pmatrix},$$

$$v_3 = \begin{pmatrix} 0.134 \\ -0.262 \\ 0.956 \end{pmatrix}.$$

From the results, the direction of v_1 is almost parallel to the *a*-axis. As for the directions of the other eigenvectors, the misalignment with the other orthogonal axes other than *a*-axis is also comparatively small.

The value of intrinsic birefringence Δn^0_{sc} for *a*-axis orientation in the PTT non-banded spherulite can be approximately estimated by the equation

$$\Delta n^0_{sc,non-banded} = \Delta n^0_a = n_X - \frac{n_Y + n_Z}{2}, \tag{9}$$

and then $\Delta n^0_{sc,non-banded} = -0.171$ was obtained. The birefringences Δn^0_c and Δn^0_{b*} for the other orthogonal axes orientation can be also calculated as follows:

$$\Delta n^0_c = n_Y - \frac{n_Z + n_X}{2},$$

$$\Delta n^0_{b*} = n_Z - \frac{n_X + n_Y}{2},$$

and then $\Delta n^0_c = 0.002$ and $\Delta n^0_{b*} = 0.169$ were obtained, respectively. The calculated value of intrinsic birefringence $\Delta n^0_{sc,non-banded}$ has a negative sign and then the result was evaluated by PLM observation of the PTT spherulite. The sign of birefringence in a spherulite is determined by the magnitude relation between the refractive index of radial direction in a spherulite n_r and that of transverse direction to radial one n_t. When the slow direction of the sensitive tint plate is parallel to the local slow direction in the spherulite, the total retardation is added and the original magenta color will change to blue color. On the contrary, when the slow direction of the sensitive tint plate is parallel to the local fast direction in the spherulite, the total retardation is compensated and the magenta color will change to orange or yellow color. Thus, blue color will be observed in the first and third quadrants and yellow color in the second and fourth quadrants for the spherulite having a positive birefringence, while the relation for the negative birefringence is opposite to the positive one. Fig. 6 shows the PLM micrographs of thinner spherulite crystallized at 140 and 190 °C. In the thinner sample of non-banded spherulite crystallized at 140 °C, the color of PLM micrograph of PTT spherulite is black and white without a sensitive tint plate (Fig. 6(a)) because of lower retardation than that in Fig. 1. On the other hand, the diagonally insertion of the sensitive tint plate between the crossed polarizing plates yielded yellow color in the first and third quadrants and blue color was in the second and fourth quadrants as shown in Fig. 6(b). It indicates that the sign of birefringence in PTT is negative ($n_r < n_t$). If the orientation direction of unit cell in the spherulite is b^*-axis, the spherulite must show positive birefringence because of the positive sign of calculated Δn^0_{b*}. Therefore, PLM result agrees with our calculation for a-axis orientation. On the other hand, the banded spherulite crystallized at 190 °C also showed negative birefringence (Fig. 6(c) and (d)). Here, if the band pattern of banded spherulite originates in the twisting of crystal lamellae [23,24] and PTT crystal lamellae takes a-axis orientation to the radial direction of the spherulite, the values of birefringence in high and low birefringent regions may be expressed as follows, respectively:

$$\Delta n^0_{sc,banded,high} = n_X - n_Z, \tag{10}$$

$$\Delta n^0_{sc,banded,low} = n_X - n_Y, \tag{11}$$

and then $\Delta n^0_{sc,banded,high} = -0.226$ and $\Delta n^0_{sc,banded,low} = -0.115$ were obtained. The signs of calculated birefringence of both high and low birefringent regions were negative and it also agrees with the result of PLM observation.

As shown in Eq. (3), the birefringence of the spherulite depends on both the crystallinity and the degree of orientation of the molecular chain in PTT crystal besides the intrinsic birefringence. Though the degree of orientation of crystal in the spherulite was not measured in this study, we can approximately estimate the birefringence of the PTT spherulite by assuming the degree of orientation as 1.0. Table 1 shows the values of birefringence for non-banded and banded spherulites estimated from Eq. (3) when the crystallinity estimated from density was adopted. The difference between calculated and observed values is not too large. The calculated intrinsic birefringence must not be so different from the real one because the crystallinity inside of the spherulite may be higher than that in bulk PTT specimen, even if the orientation function is not estimated. Moreover, the fractional atomic coordinates used to calculate the intrinsic birefringence is that of PTT fiber [17] and then the coordinates may be different in some degree from that of the spherulite. However, it must not too large because the lattice constant of the spherulite is not so different from that of the fiber [26].

In the PTT banded spherulite, it is believed that the band is composed of twisting lamella and the periodic interference color under PLM originates in the existence of flat-on and edge-on lamellae. From our calculated result, it is suggested that the absolute value of birefringence in flat-on lamella Δn (ab^* plane) is higher than that of edge-on lamella Δn (ac plane). Chuang et al. [27] reported both atomic force microscope (AFM) image and a monochrome PLM image of PTT banded

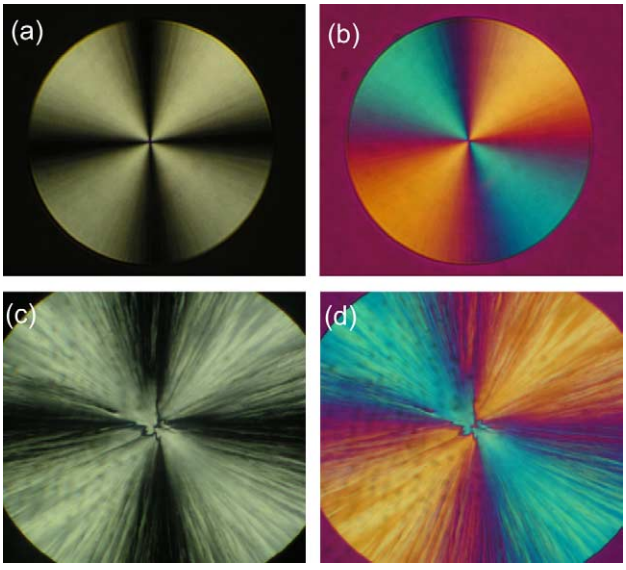

Fig. 6. PLM images of PTT thinner spherulites crystallized at (a), (b) T_{iso} = 140 °C and (c), (d) 190 °C (sample thickness is about 1 μm) (a), (c) without a sensitive tine plate and (b), (d) with a sensitive tint plate.

Table 1
Calculated and observed values of birefringence in PTT spherulite

	Birefringence	
	Calculated value	Observed value
Non-banded spherulite crystallized at 140 °C	−0.038	−0.044
Banded spherulite crystallized at 190 °C	−0.059	−0.060
	−0.030	−0.043

spherulite, and the edge-on lamellae observed under AFM corresponded to the dark bands under PLM (lower birefringence region) while the terrace-like lamellae to the bright bands (higher birefringence region). Our calculated result shows good agreement with their observation.

4. Conclusion

When PTT was isothermally melt-crystallized, the colorful spherulite was observed under crossed polarizer condition without a sensitive tint plate because of its high retardation. The direction of crystal axes in the spherulite was estimated by the small area X-ray diffraction measurement, which is necessary information to calculate the birefringence in PTT spherulite. It was verified that *a*-axis is almost parallel to the radial direction of the PTT spherulite.

Based on the result, the birefringence Δn_{sc}^{0} in the PTT spherulite was calculated and then much higher value than the intrinsic birefringence for *c*-axis orientation in the PTT fiber was obtained. Moreover, in our calculation, it became clear that the refractive index for *a*-axis direction is smallest in the orthogonal three directions and the absolute value of intrinsic birefringence for *a*-axis orientation is high, while that for *c*-axis orientation is considerably low. It is the reason why the PTT spherulite has the high birefringence. Moreover, the calculated birefringence shows good agreement with observed results.

Acknowledgements

The authors appreciate Prof S. Asai (Tokyo Institute of Technology) for making the software for us to analyze the data of small area X-ray diffraction and for discussion. We are also indebted to Dr S. Umemoto (Tokyo Institute of Technology) for advice on the calculation of refractive indices.

References

[1] Poulin-Dandurand S, Perez S, Revol JF, Brisse F. Polymer 1979;20:419–26.
[2] Ho RM, Ke KZ, Chen M. Macromolecules 2000;33:7529–37.
[3] An JB, Saito H, Inoue T, Ougizawa T, Kim BS. Kobunshi Nonbunshu 1999;(56):635–8.
[4] Geil PH. Polymer single crystals. New York: Wiley; 1963.
[5] Bassett DC. Principles of polymer morphology. Cambridge: Cambridge University Press; 1981.
[6] Grebowicz JS, Brown H, Chuah H, Olvera JM, Wasiak A, Sajkiewicz P, et al. Polymer 2001;42:7153–60.
[7] Lyoo WS, Lee HS, Ji BC, Han SS, Koo K, Kim SS, et al. Appl Polym Sci 2001;81:3471–80.
[8] Frisk S, Ikeda RM, Chase DB, Kennedy A, Rabolt JF. Macromolecules 2004;37:6027–36.
[9] Wu J, Schultz JM, Samon JM, Pangelinan AB, Chuah HH. Polymer 2001; 42:7141–51.
[10] Garg SK. J Appl Polym Sci 1982;27:2857–67.
[11] Gupa VB, Kumar M, Gulrajani LM. Text Res J 1975;45:463.
[12] Chuah HH. J Polym Sci, Part B: Polym Phys 2002;40:1513–20.
[13] Kim KJ, Bae JH, Kim YH. Polym Int 2003;52:35–41.
[14] Hong PD, Chung WT, Hsu CF. Polymer 2002;43:3335–43.
[15] BaltaCallleja FJ, Vonk CG. X-ray scattering of synthetic polymers. Amsterdam: Elsevier; 1989.
[16] Wunderlich B. Macromolecular physics, vol. 1. New York: Academic Press; 1973 p. 385.
[17] Desborough IJ, Hall IH, Neisser JZ. Polymer 1979;20:545–52.
[18] Chuah HH. Macromolecules 2001;34:6985–93.
[19] Wang B, Li CY, Hanzlicek J, Cheng SZD, Geil PH, Grebowicz J, et al. Polymer 2001;(42):7171–80.
[20] Lorentz HA. Ann Phys 1880;9:641–65.
[21] Lorenz LV. Ann Phys 1880;11:70–103.
[22] Ohkoshi Y, Nagura M. Sein'I Gakkaishi 1993;49:601–4.
[23] Keller A. J Polym Sci 1955;17:291–308.
[24] Keith HD, Padden Jr FJ. J Polym Sci 1959;39:101–22.
[25] Bunn CW. Chemical crsytallography. New York: Oxford University Press; 1961 [chapter 8].
[26] Yang J, Sidoti G, Liu J, Geil PH, Li CY, Cheng SZD. Polymer 2001;42: 7181–95.
[27] Chuang WT, Hong PD, Chuah HH. Polymer 2004;45:2413–25.